Primary cilia regulate mandibular development

Atsushi Kitamura

Division of Oral and Maxillofacial Surgery, Department of Health Science, Course for Oral science, Niigata University Graduate School of Medical and Dental Sciences, Niigata, Japan

ABSTRACT

The primary cilia play a critical role in many biological processes including bone and cartilage formation. Perturbations in the function of primary cilia are known to cause a wide spectrum of human diseases: the ciliopathies. Craniofacial dysmorphologies including mandibular deformity are often seen in patients with ciliopathies. Mandibular development is characterized by chondrogenesis and osteogenesis. However, it remains unclear whether the primary cilia are involved in mandibular development. To address this question, we generated mice with a mesenchymal deletion of ciliary protein, *Ift88* (*Ift88*$^{fl/fl}$*;Wnt1Cre*) and *Ofd1* (*Ofd1*^{fl}*;Wnt1Cre*). Both *Ofd1* and *Ift88* mutant mice showed ectopic mandibular bone, which was found to be associated with the downregulation of Shh signaling. Unlike mandibular bone, Meckel's cartilage showed different phenotypes between *Ofd1*^{fl}*;Wnt1Cre* and *Ift88*$^{fl/fl}$*;Wnt1Cre* mice. Bifurcated and enlarged Meckel's cartilage were observed in the posterior mandible of *Ofd1*^{fl}*;Wnt1Cre* mice, whereas *Ift88*$^{fl/fl}$*;Wnt1Cre* mice exhibited enlarged Meckel's cartilage in the entire mandible. Chondrogenesis and osteogenesis during mandibular development is thus regulated by the primary cilia, and each ciliary protein is likely to have a distinct role, depending on the regions.

INTRODUCTION

Understanding molecular mechanisms during jaw development is crucial, as approximately one-third of all the congenital defects show craniofacial anomalies, including micrognathia. Mandibular development relies on chondrogenesis and osteogenesis. Meckel's cartilage is believed to act as a transient supportive tissue for mandibular bone formation during embryogenesis, which disappears at late gestation and/or the neonatal stage of development. Meckel's cartilage initiates in the mandibular process at the molar tooth region and then extends to both directions along the anterior–posterior axis. Mandibular bone is first seen as condensed mesenchymal cells that proliferate and differentiate into osteogenic cells. The ossification of the mandibular bone mainly begins in the mesenchyme buccal to Meckel's cartilage at the molar tooth region, and the developing mandibular bone then surrounds Meckel's cartilage. However, except in the incisor region, most of the mandibular bone forms in the mesenchyme buccal to Meckel's cartilage, and only a thin portion of the bone is formed in the mesenchyme lingual to Meckel's cartilage. Mandibular development is known to be regulated by epithelial–mesenchymal interactions (MacDonald and Hall 2001, Havens et al., 2006, Paiva et al., 2010). Mandibular development, including mandibular bone and Meckel's cartilage formation, has been shown to be regulated by complex molecular mechanisms; however, these are not fully understood (Liu et al., 2010, Zhang et al., 2011, Wang et al., 2013, Parada and Chai 2015).

The primary cilium is a nonmotile organelle existing on the surface of almost all somatic cells in vertebrates. It has been shown to play critical roles in many biological processes, such as determining left/right axis patterning and sensory functions, including sensing to light, odor, fluid flow, osmolarity changes, and sound, as well as in regulating signaling pathways (Evans et al., 2006, Bisgrove and Yost 2006, Zaghloul and Brugmann 2011). Shh signaling is known to be activated within the primary cilia. The primary cilium comprises a membrane-bound cylinder surrounding nine doublet microtubules that extend from a basal body. The basal body is derived from the mother centriole of the centrosome. Cilia are assembled and maintained by intraflagellar transport (IFT) system, in which multiple protein complexes bidirectionally move along the axoneme by the coordinated action of IFT motors. In IFT, groups of protein particles are transported from the base to the tip of the cilia (anterograde) by kinesin-II and from the tip to the base (retrograde) by cytoplasmic dynein 1b. IFT particles comprise at least 17

polypeptides, which form two complexes, namely complex A and B (Cole, 2003; Eggenschwiler and Anderson 2007). IFT are a highly conserved system in all ciliated eukaryotic cells, and perturbations in the function of primary cilia are implicated in a wide spectrum of human diseases: the ciliopathies (Rosenbaum and Witman, 2002; Pan et al., 2005; Bisgrove and Yost. 2006; Evans et al., 2006, Hennekam et al., 2010). Mandibular abnormalities, including micrognathia, are observed as one of the symptoms in many ciliopathy patients (Hennekam et al., 2010, Zaghloul and Brugmann 2011). The primary cilia has also been shown to be involved in chondrogenesis and osteogenesis (Yuan and Yang 2016). However, the role of the primary cilia in mandibular development remains unknown.

Ift88 encodes a protein that is required for IFT and the primary cilia formation (Murcia et al., 2000). *Ofd1* encodes a protein that localizes in the basal body of the primary cilia (Ferrante et al., 2006). To understand the role of the primary cilia in mandibular development, we generated mice with tissue conditional deletions of *Ift88* and *Ofd1*. By analyzing these mutants, the primary cilia in the mesenchyme regulates mandibular development through controlling chondrogenesis and osteogenesis.

MATERIALS & METHODS

Production and analysis of transgenic mice

Ift88$^{fl/fl}$, *Ofd1*$^{fl/fl}$, *Wnt1Cre*, *Sox9Cre* and *K14Cre* mice were produced as described by Haycraft et al., 2007, Ferrante et al., 2006, Danielian et al. (1998), Akiyama et al., (2005) and Yi et al. (2006), respectively. We also used *Gli3*^{Xt} (Xt^J; Takahashi et al., 1998) mice as *Gli3* mutants. Embryonic day 0 (E0) was taken to be midnight prior to finding a vaginal plug.

Cell proliferation

For detection of cell proliferation, pregnant females were injected intraperitoneally with BrdU (Roche) labeling reagent (45 mg/g body weight) at E12.5. One hour after injection, embryos were fixed in 4% PFA fixative and embedded in paraffin wax, from which sections were cut. Immunodetection of BrdU was performed using the BrdU labeling and detection kit (Roche) according to manufacturer's instructions.

In situ hybridization

Section or whole mount *in situ* hybridization was carried out as described previously (Ohazama et al., 2008).

Immunohistochemistry

After deparaffinization, sections were treated with proteinase K and then incubated with antibodies to Phosphorylated Smad1, Smad5 and Smad8 (p-Smad1/5/8; Cell Signaling Technology) and Gli2 (Proteintech). Tyramide signal amplification system (Parkin Elmer Life Science) was performed for detecting the p-Smad1/5/8 antibody.

Skeletal Preparation

To analyze the skeleton, pups were stained with Alcian blue for nonmineralized cartilage and Alizarin Red for bone. Briefly, mice were fixed in 100% ethanol and then stained for 5 days in 0.1% Alizarin Red S (in 95% ethanol), 0.3% Alcian blue (in 70% ethanol), 100% acetic acid, and ethanol, followed by alkaline hydrolysis and glycerol clearing.

3D reconstruction of Meckel's cartilage

The 3D reconstructions of Meckel's cartilage were made from serial sections as described

previously (Kawasaki et al., 2014) using the AMIRA software package (Template Graphics Software).

Q-PCR analysis

Mouse embryo heads were embedded in Optimal cutting temperature compound (Sakura Finetek), serially sectioned at 10 μm and stained with 0.02% toluidine blue. Mesenchyme lingual to Meckel's cartilage was dissected out with laser microdissection (Leica). Total RNA was isolated from the tissues according to the manufacturer's protocol of the RNeasy Mini Kit (Qiagen). Total RNA was then randomly primed for cDNA synthesis using the TransPlexH Complete Whole Transcriptom Amplification Kit (Sigma-Aldrich). Q-PCR was performed using GoTaq qPCR Master Mix (Promega) with the carboxy-X-rhodamine (CXR) Dye and Rotor-Gen-Q (Qiagen) detection system. All samples were run in triplicate for each experiment, and relative transcript abundance was normalized to the amount of GAPDH. Primer sequences for *Gli2* are forward: 5'-TACCTCAACCCTGTGGATGC, and reverse: 5'- CTACCAGCGAGTTGGGAGA.

RESULTS

Epithelial Ofd1 and Ift88 in mandibular development

Conventional mutations of *Ofd1* or *Ift88* has been shown to lead to early embryonic lethality (approximately E7.5; Murcia et al., 2000, Ferrante et al., 2006). Therefore, mice with tissue conditional *Ofd1* or *Ift88* mutations were generated using the Cre-LoxP system. We firstly generated and examined mice with epithelial conditional *Ofd1* or *Ift88* mutations using *Keratin(K)14Cre* (*Ofd1^{fl};K14Cre*, *Ift88$^{fl/fl}$;K14Cre*). We used hemizygous *Ofd1* mutant mice as conditional *Ofd1* knockout mice, since *Ofd1* is located on the X chromosome. Neither *Ofd1^{fl};K14Cre* nor *Ift88$^{fl/fl}$;K14Cre* showed significant changes in the mandible (data not shown).

Bone formation in Ofd1 and Ift88 mutant mice

We next generated mice with the conditional loss of *Ift88* and *Ofd1* on neural crest-derived cells using *Wnt1Cre* (*Ofd1^{fl};Wnt1Cre*, *Ift88$^{fl/fl}$;Wnt1Cre*). Both *Ift88$^{fl/fl}$;Wnt1Cre* and *Ofd1^{fl};Wnt1Cre* mice died at birth due to the presence of cleft palate. The mandibles of these mutants were slightly shorter than those of wild-type mice (Millington et al., 2017). Excess formation of mandibular bone lingual to Meckel's cartilage (lingual mandibular bone) was observed in both *Ofd1^{fl};Wnt1Cre* and *Ift88$^{fl/fl}$;Wnt1Cre* mice, whereas endogenous mandibular bone (mandibular bone buccal to Meckel's cartilage) showed no significant changes (Fig. 1B, 1C, 1E, 1F). In both mutants, ectopic condensed mesenchyme was observed in the region corresponding to the lingual mandibular bone from E12.5, which showed the excess expression of the osteoblast differentiation marker, *Runx2* (Fig. 1H, 1I, 1K, 1L). Abnormal mandibular bone formation in *Ofd1* and *Ift88* mutants was observed to be fully penetrant (14/14). To understand whether the excess lingual mandibular bone was ectopic bone or expanded bone from endogenous mandibular bone, we examined cell proliferation by a BrdU assay. Ectopic cell proliferation was observed in the region lingual to Meckel's cartilage, which was found to be isolated from the endogenous mandibular bone region (Fig. 1N, 1O, data not shown). Excess lingual mandibular bone is thus likely to be caused by ectopic bone formation.

To identify candidate molecules related to mandibular bone phenotypes in *Ofd1^{fl};Wnt1Cre* and *Ift88$^{fl/fl}$;Wnt1Cre* mice, we performed *in situ* hybridization and immunohistochemistry analysis at E12.5 when ectopic condensed mesenchyme and *Runx2* expression were evident in

mutants. It has been shown that Fgf, Wnt and Bmp signaling pathways are related to craniofacial development, including mandibular development (Mina et al., 2007, Havens et al., 2007, Brugmann et al., 2007, Vendrell et al., 2009, Terao et al., 2011, Bonilla-Claudio et al., 2012, Komatsu 2013,). Neither *Ift88*$^{fl/fll}$*;Wnt1Cre* nor *Ofd1*$^{f/l}$*;Wnt1Cre* mice exhibited significant differences in the expression of *Etv5* (a marker of Fgf signaling) and *Axin2* (a transcriptional target of the canonical Wnt signaling pathway), and the immunoreaction of phosphorylated Smad1, Smad5 and Smad9 (p-Smad1/5/9; a marker of Bmp signaling; data not shown).

Since Shh signaling is known to be activated within the primary cilia and is involved in craniofacial development, *Ptch1* expression (a direct target of hedgehog signaling) was examined in both *Ift88*$^{fl/fll}$*;Wnt1Cre* and *Ofd1*$^{f/}$*;Wnt1Cre* mice (Evans et al., 2006, Bisgrove and Yost 2006, Zaghloul and Brugmann 2011, Adel Al-Lami et al., 2016). *Ptch1* expression was observed in wild-type mesenchyme corresponding to mutant condensed mesenchymal cells from E11, which was significantly down-regulated in both *Ofd1* and *Ift88* mutant mandibles (Fig. 2A-2C, data not shown). To further confirm whether region showsing *Ptch1* expression is involved in bone formation in mutant mandible lingual to Meckel's cartilage, we also generated *Ofd1*$^{f/}$*;Sox9Cre* mice, since *Sox9* expression was found to be overlapped with *Ptch1* expression in wild-type mesenchyme corresponding to mutant condensed mesenchymal cells from E11.5 (Fig. 2D, data not shown). *Sox9* is also known to be expressed in osteoprecursor cells (Akiyama et al., 2005). In common with *Ofd1*^{fl}*;Wnt1Cre* and *Ift88*$^{fl/fl}$*;Wnt1Cre* mice, excess lingual mandibular bone was observed in *Ofd1*$^{f/}$*;Sox9Cre* mice (Fig. 2E). To further understand Shh signaling in mutant ectopic lingual mandibular bone formation, we analyzed the expression of transcription factors in Shh signaling, *Gli1*, *Gli2*, and *Gli3*. Unlike *Ptch1*, *Gli1* expression could not be detected in mesenchyme lingual to Meckel's cartilage in wild-type mice (Fig. 2F). No ectopic *Gli1* expression was observed in mandibles of both mutants, whereas *Gli1* expression in endogenous mandibular bone was reduced in both mutants (Fig. 2G, 2H). In wild-type mice, weak immunolocalization of Gli2 was observed in mesenchyme lingual to Meckel's cartilage, while *Gli3* was expressed in the similar region (Fig. 2I, 2L). Gli2 immunoreaction and *Gli3* expressions were found to be down-regulated in both mutants, which were confirmed by qPCR analysis using RNA obtained by laser microdissection (Fig. 2J, 2K, 2M, 2N, data not shown).

In order to investigate whether extra lingual mandibular bone formation in mutant mice is caused by the changes of Shh signaling pathway, we generated mice with a mesenchymal

conditional mutation of *Smo* (a Shh signaling essential molecule) using *Wnt1Cre* mice (*Smo$^{fl/fl}$;Wnt1Cre*; Jeong et al., 2004, Billmyre and Klingensmith 2015). In this mutant, Shh signaling is down-regulated in mesenchyme due to a lack of activator isoform of GLIs (Both GLI2 and GLI3 are known to function as either an activator or repressor isoforms, while GLI1 act as only activator isoform. Smo inhibits the production of repressor GLI isoform.: Jeong et al., 2004, Corbit et al., 2005 Kim et al., 2009, Sasai and Briscoe, 2012, Falkenstein and Vokes 2014, Millington et al., 2017). It has been shown that *Smo* mutants exhibit obvious small lower jaws (Jeong et al., 2004). In common with *Ofd1^{fl};Wnt1Cre* and *Ift88$^{fl/fl}$;Wnt1Cre* mice, excess lingual mandibular bone was observed in *Smo$^{fl/fl}$;Wnt1Cre*, whereas the thickness of endogenous mandibular bone showed no obvious changes (Fig. 2P, 2R). Moreover, similar to that in *Ift88* and *Ofd1* mutants, the ectopic condensation of mesenchymal cells and *Runx2* expression were observed in mesenchyme lingual to Meckel's cartilage in *Smo* mutants at E12.5 and E13.5 (Fig. 2T, data not shown). These data suggested that the lack of Shh signaling in mesenchyme lingual to Meckel's cartilage is likely to cause ectopic bone formation in *Ofd1^{fl};Wnt1Cre* and *Ift88$^{fl/fl}$;Wnt1Cre* mice. We also examined *Gli3* mutants, since *Gli3* expression was significantly down-regulated in both *Ift88* and *Ofd1* mutants. However, *Gli3* mutants showed no significant abnormal mandibular bone formation (Fig. 3).

Meckel's cartilage formation in Ofd1 and Ift88 mutants

Extra Meckel's cartilage was observed in the posterior mandible of *Ofd1^{fl};Wnt1Cre* mice at E18.5 (9/14, Fig. 4B). By the analysis of 3D reconstruction of Meckel's cartilage from histological specimens, the ectopic cartilage formation was found to be caused by the bifurcation of Meckel's cartilage (Fig. 4E). Meckel's cartilage was bifurcated from the molar region to posterior region. The posterior region of Meckel's cartilage was slightly enlarged in *Ofd1* mutants, whereas its anterior region showed no obvious anomalies. Unlike *Ofd1* mutants, the enlargement of Meckel's cartilage was observed in the entire mandible of *Ift88* mutants, while bifurcation of Meckel's cartilage was not observed in *Ift88* mutants (Fig. 4F). These cartilage phenotypes became apparent in both mutants from E13.5. The perichondrium of the Meckel's cartilage was evident in wild-type mandible from E13.5, which was found to be thickened in the posterior mandible of *Ofd1* mutants and the entire mandible in *Ift88* mutants (Fig. 4H, 4I). To identify candidate molecules related to cartilage phenotypes in *Ofd1^{fl};Wnt1Cre* and *Ift88$^{fl/fl}$;Wnt1Cre* mice, we performed *in situ* hybridization and immunohistochemistry analysis at E13.5. P-Smad1/5/9 immunolocalization, and *Erm* and *Axin2* expression around

mutant Meckel's cartilage showed no significant changes, suggesting that Bmp, Fgf, and Wnt are unlikely to be involved in Meckel's cartilage phenotype in *Ofd1*$^{fl/Y}$*;Wnt1Cre* and *Ift88*$^{fl/fl}$*;Wnt1Cre* mice (data not shown). Unlike ectopic lingual mandibular bone formation, no significant changes in *Gli3* expression were observed in mesenchyme around Meckel's cartilage, whereas *Gli1* expression and Gli2 immunoreaction were obviously down-regulated in the pericondrium of both mutant mice (Fig. 5A-5I). *Smo*$^{fl/fl}$*;Wnt1Cre* mice showed enlarged Meckel's cartilage without bifurcation, although cartilage in *Smo* mutants was obviously shorter than that in *Ofd1*$^{fl/Y}$*;Wnt1Cre* and *Ift88*$^{fl/fl}$*;Wnt1Cre* mice (Fig. 5K, 5M). Neither extra Meckel's cartilage nor bifurcation of Meckel's cartilage could be detected in *Ofd1*$^{f/}$*;Sox9Cre* mice, although Sox9 is expressed in chondroprogenitor cells (Fig. 5O; Akiyama et al., 2005).

Posterior structure of mandibles in Ofd1 and Ift88 mutants

In wild-type mice, developing mandibular bone extends along the anterior–posterior axis, and then the posterior end of the mandible starts to form three mandibular processes, condylar, coronoid, and angular, which are classified as the secondary cartilage. It has been shown that these cartilages are derived from the periosteum of the ossifying mandible in mammals (Symons 1952, Bhaskar 1953, Meikle 1973, Shibata et al., 1996, Shibata et al., 1997, Fukada et al., 1999, Fukuoka et al., 2007, Shibata et al., 2013). To understand whether ectopic lingual bone formation also leads to the formation of the posterior structure of the mandible, we examined the posterior end of mutant mandibles. In wild-type mice, cartilage is observed only in the angular and condylar processes at birth (Fig. 6A). Extra cartilage formation was observed in all *Smo*, *Ift88*, and *Ofd1* mutants, which corresponded to the ectopic mandibular bone region (Fig. 5B-5D). These extra cartilage formation was isolated from other endogenous cartilage (the angular and condylar processes) at the posterior end of mutant mandibles, supporting that mandibular bone phenotype in mutants wasd caused by ectopic bone formation, but not expanding from endogenous mandibular bone. These findings also indicate that the mutant lingual bone formation programmed as mandibular bone. It has been shown that there is an interaction between condylar and glenoid fossa formation (Wang et al., 2011). To determine whether abnormal posterior mandibular formations in mutants affect glenoid fossa development, we examined the temporal bone region of mutants. All *Ofd1*, *Ift88,* and *Sm*o mutants lacked the glenoid fossa formation (Fig. 5F-6H, data not shown).

Ossicle formation in Ofd1 and Ift88 mutants

Neural crest-derived cells and cartilages in branchial arches are known to be involved in the development of middle ear apparatus (ossicles; malleus, incus, and stapes; Thompson et al., 2012, Thompson and Tucker 2013). To investigate whether the primary cilia regulate ossicle formation, we examined the ossicles of *Ift88* and *Ofd1* mutants. Abnormal ossicle formation was observed in all *Smo*, *Ift88*, and *Ofd1* mutants (Fig. 6J-6L).

Genetic interaction between Ift88 and Ofd1mutants

Ift88 mutant mandibular phenotypes were thus similar to *Ofd1* mutant phenotypes. To investigate potential genetic interactions between *Ofd1* and *Ift88* in mandibular development, we intercrossed *Ift88* mutants with *Ofd1* mutants. *Ift88*$^{fl/fll}$*;Ofd1*^{fl}*;Wnt1Cre* mice showed no exacerbation or attenuation of the mandibular bone formation in comparison with those in *Ofd1*$^{fl/Y}$*;Wnt1Cre* and *Ift88*$^{fl/fl}$*;Wnt1Cre* mice (Fig. 7). However, no ectopic Meckel's cartilage was observed in *Ift88*$^{fl/fll}$*;Ofd1*^{fl}*;Wnt1Cre* mice.

DISCUSSION

Ofd1^{fl}*;Wnt1Cre* and *Ift88*$^{fl/fl}$*;Wnt1Cre* mice exhibited extra lingual mandibular bone formation, suggesting that the primary cilia are likely to inhibit bone formation in wild type mandible corresponding to the region showing extra lingual mandibular bone formation in mutants. In fact, the deletion of another ciliary protein, *Kif3a*, has also been reported to lead to ectopic bone formation in the craniobase (Koyama et al., 2007). Shh signaling was down-regulated in mesenchyme lingual to Meckel's cartilage in both *Ofd1*^{fl}*;Wnt1Cre* and *Ift88*$^{fl/fl}$*;Wnt1Cre* mice, and similar mandibular bone phenotypes of *Ift88* and *Ofd1* mutants were observed in *Smo*$^{fl/fl}$*;Wnt1Cre* mice. These findings suggest that extra mandibular bone formation in *Ofd1* and *Ift88* mutants was caused by the lack of Shh signaling. *Ofd1* and *Ift88* thus regulate mandibular bone formation through Shh signaling. *Gli2* and *Gli3* expressions were observed in wild-type mesenchyme corresponding to the ectopic mandibular bone formation, which were down-regulated in *Ofd1* and *Ift88* mutants. In contrast, *Gli1* expression was not detected in the region of either wild-type or *Ofd1* and *Ift88* mutants, indicating that mandibular bone formation lingual to Meckel's cartilage is regulated by Shh signaling through *Gli2* and *Gli3*. Although *Gli2* and *Gli3* expressions were down-regulated in mesenchyme corresponding to the ectopic mandibular bone formation in *Ofd1* and *Ift88* mutants, ectopic mandibular bone formation was not observed in *Gli3* mutants. It has been shown that the double mutation of *Glis*, such as *Gli2* and *Gli3* or *Gli1* and *Gli2*, lead to developmental anomalies, whereas single deletion of *Gli* did not show these phenotypes (Park et al., 2000, Hardcastle et al., 1998, Millington et al., 2017). It is possible that the ectopic mandibular bone formation was caused by the lack of both *Gli2* and *Gli3* expressions. Unlike ectopic bone formation in both mutants (*Ofd1*^{fl}*;Wnt1Cre* and *Ift88*$^{fl/fl}$*;Wnt1Cre*), no significant changes of endogenous mandibular bone (buccal to Meckel's cartilage) were found in these mutants, although *Ptch1*, *Gli1*, *Gli2*, and *Gli3* expressions were observed in the endogenous mandibular bone region in wild-type mice, which were altered in *Ift88* and *Ofd1* mutants. *Smo*$^{fl/fl}$*;Wnt1Cre* mice showed no significant anomalies of the endogenous mandibular bone formation, suggesting that Shh signaling is dispensable for endogenous mandibular bone formation.

In addition to ectopic bone formation, enlarged Meckel's cartilage was observed in the entire mandible of *Ift88*$^{fl/fl}$*;Wnt1Cre* mice. Shh signaling was down-regulated in the perichondrium around Meckel's cartilage in *Ift88*$^{fl/fl}$*;Wnt1Cre* mice, and similar Meckel's cartilage phenotypes

of *Ift88* mutants were observed in *Smo$^{fl/fl}$;Wnt1Cre* mice. Enlarged Meckel's cartilage and downregulation of Shh signaling were also observed in the posterior mandible of *Ofd1* mutants, suggesting that the primary cilia is likely to regulate Meckel's cartilage formation through Shh signaling. Contrary to the mandibular bone formation, no significant changes in *Gli3* expression were observed in *Ift88* or *Ofd1* mutants. On the other hand, *Gli1* and *Gli2* expression were observed in the wild-type perichondrium, which was down-regulated in *Ofd1* and *Ift88* mutants. Meckel's cartilage is thus regulated by Shh signaling through *Gli1* and *Gli2*, but not *Gli3*. These data suggest that mandibular bone and Meckel's cartilage formation are regulated by Shh signaling through different Glis. Although Shh signaling was altered in the perichondrium around Meckel's cartilage of *Ofd1* mutants, only posterior Meckel's cartilage was enlarged in *Ofd1* mutants, and the anterior Meckel's cartilage of *Ofd1* mutants showed no obvious phenotypes. It is likely that other molecular changes in *Ofd1* mutants rescue the anterior Meckel's cartilage formation from the lack of Shh signaling. The bifurcation of Meckel's cartilage in the posterior mandible of *Ofd1* mutants suggests that *Ofd1* is involved in regulating the direction of Meckel's cartilage formation, which is restricted in the posterior mandible. Furthermore, the bifurcation of Meckel's cartilage was never observed in *Ift88$^{fl/fl}$;Wnt1Cre* mice, indicating that in Meckel's cartilage formation, *Ofd1* plays a role distinct from that of *Ift88*. Moreover, the bifurcation of Meckel's cartilage found in *Ofd1$^{f/}$;Wnt1Cre* mice could not be detected in *Ofd1$^{f/}$;Sox9Cre* mice, suggesting that the direction of Meckel's cartilage formation is unlikely to be determined by *Ofd1* in chondroprogenitor cells.

Mandibular bone phenotypes in *Ift88$^{fl/fl}$;Wnt1Cre* mice were identical to those in *Ofd1^{fl};Wnt1Cre* mice. Furthermore, double mutations of *Ofd1* and *Ift88* resulted in no exacerbation or attenuation of mandibular bone phenotypes. These findings suggest that mechanisms underlying *Ofd1* function are similar to those underlying *Ift88* function in mandibular bone development. It has been shown that Ofd1 recruits Ift88 for regulating centriole and subsequent the primary cilia formation (Singla et al., 2010). It is likely that either *Ofd1* or *Ift88* deletion compromise these events, resulting in the same mandibular bone phenotype. However, unlike mandibular bone formation, bifurcated Meckel's cartilage was observed in *Ofd1* mutants, which could not be detected in *Ift88$^{fl/fll}$;Ofd1^{fl};Wnt1Cre* mice. It is possible that there is genetic interaction between *Ofd1* and *Ift88* in Meckel's cartilage formation,

although the function in Meckel's cartilage development is likely to be different between *Ofd1* and *Ift88*.

All mutant mice (*Ofd1^{fl};Wnt1Cre*, *Ofd1^{fl};Sox9Cre*, *Ift88$^{fl/fl}$;Wnt1Cre* and *Smo$^{fl/fl}$;Wnt1Cre*) lacked the glenoid fossa, and showed extra posterior cartilage process formation. It has been shown that there is interaction between glenoid fossa and condyle development, and proper signals from the developing condyle or Meckel's cartilage are required for glenoid fossa development (Wang et al., 2011). Thus, the lack of glenoid fossa formation is likely to be caused by abnormal mandibular formation.

OFD1 was identified as the mutated gene in patients with Oral-facial-digital type I (OFD1) syndrome. OFD1 syndrome is characterized by malformations of the oroface and digitals regions (Gurrieri et al., 2007; Franco 2008; Macca and Franco 2009). Micrognathia has been shown to be observed in Ofd1 patients, which was also observed in *Ofd1^{fl};Wnt1Cre* mice in this study. However, ectopic mandibular bone formation has not been reported in Ofd1 syndrome patients. Thus, the role of *Ofd1* in mandibular development is slightly different between humans and mice.

Acknowledgements

This research was funded by the Japan Society for the Promotion of Science (JSPS; 16H05539E). We would like to thank Prof. Yamada for providing *Gli3* mutants. I would like to thank Professors Ritsuo Takagi and Atsushi Ohazama for their critical reading and valuable comments on this manuscript. I also thank the Oral Anatomy Department staff for their technical assistance.

REFERENCES

Akiyama H, Kim JE, Nakashima K, Balmes G, Iwai N, Deng JM, Zhang Z, Martin JF, Behringer RR, Nakamura T, de Crombrugghe B. Osteo-chondroprogenitor cells are derived from Sox9 expressing precursors. Proc Natl Acad Sci U S A. 2005 Oct 11;102(41):14665-70.

Adel Al-Lami H, Barrell WB, Liu KJ. Micrognathia in mouse models of ciliopathies. Biochem Soc Trans. 2016 Dec 15;44(6):1753-1759

Bhaskar SN. 1953. Growth pattern of the rat mandible from 13days insemination age to 30days after birth. Am J Anat 92(1):1-53..

Billmyre KK, Klingensmith J. 2015. Sonic hedgehog from pharyngeal arch 1 epithelium is necessary for early mandibular arch cell survival and later cartilage condensation differentiation. Dev Dyn. 244(4):564-76.

Bisgrove BW, Yost HJ. 2006. The roles of cilia in developmental disorsers and disease. Development. 133(21):4131-43.

Bonilla-Claudio M1, Wang J, Bai Y, Klysik E, Selever J, Martin JF. 2012. Bmp signaling regulates a dose-dependent transcriptional program to control facial skeletal development. Development. 139(4):709-19

Brugmann SA, Goodnough LH, Gregorieff A, Leucht P, ten Berge D, Fuerer C, Clevers H, Nusse R, Helms JA. 2007. Wnt signaling mediates regional specification in the vertebrate face. Development. 134(18):3283-95.

Cole DG. 2003. The intraflagellar transport machinery of Chlamydomonas reinhardtii. Traffic. 4(7):435-442.

Corbit, K.C., Aanstad, P., Singla, V., Norman, A.R., Stainier, D.Y., Reiter, J.F., 2005. Vertebrate Smoothened functions at the primary cilium. Nature 437, 1018–1021.

Danielian PS, Muccino D, Rowitch DH, Michael SK, McMahon AP. 1998. Modification of gene activity in mouse embryos in utero by a tamoxifen-inducible form of Cre recombinase. Curr Biol. 3;8(24):1323-6

Eggenschwiler JT, Anderson KV. Cilia and developmental signaling. 2007. Annu Rev Cell Dev Biol. 23:345-373.

Evans JE, Snow JJ, Gunnarson AL, Ou G, Stahlberg H, McDonald KL, Scholey JM. 2006. Functional modulation of IFT kinesins extends the sensory repertoire of ciliated neurons in Caenorhabditis elegans. J Cell Biol. 172(5):663-669.

Falkenstein KN, Vokes SA. 2014. Transcriptional regulation of graded Hedgehog signaling.

Semin Cell Dev Biol. 33:73-80.

Ferrante MI, Zullo A, Barra A, Bimonte S, Messaddeq N, Studer M, Dollé P, Franco B. 2006. Oral-facial-digital type I protein is required for primary cilia formation and left-right axis specification. Nat Genet. 38(1):112-7.

Franco, B. The molecular basis of oral-facial-digital type I (OFDI) syndrome. In: Epstein, J.C., Erickson, R.P., Wynshaw-Boris, A. (Eds.), Inborn Errors of Development, Vol. I, Chaptr 156. Oxford University Press, New York, pp. 1379-1386, 2008.

Fukada K, Shibata S, Suzuki S, Ohya K, Kuroda T. 1999. In situ hybridization study of type I, II, X collagens and aggrecan mRNAs in the developing condylar cartilage of fetal mouse mandible. J Anat 195 (Pt 3):321-9.

Fukuoka H, Shibata S, Suda N, Yamashita Y, Komori T. 2007. Bone morphogenetic protein rescues lack of secondary cartilage in Runx2-deficient mice. J Anat 211(1):8-15.

Gurrieri F, Franco B, Toriello H, Neri G. 2007. Oral-facial-digital syndromes: review and diagnostic guidelines. Am J Med Genet A. 15;143A(24):3314-23..

Hardcastle Z1, Mo R, Hui CC, Sharpe PT. 1998. The Shh signalling pathway in tooth development: defects in Gli2 and Gli3 mutants. Development. 125(15):2803-11.

Havens BA, Rodgers B, Mina M. 2006. Tissue-specific expression of Fgfr2b and Fgfr2c isoforms, Fgf10 and Fgf9 in the developing chick mandible. Arch Oral Biol. 51(2):134-45.

Haycraft CJ; Zhang Q; Song B; Jackson WS; Detloff PJ; Serra R; Yoder BK. 2007. Intraflagellar transport is essential for endochondral bone formation. Development 134(2):307-316.

Hennekam RCM, Krantz I, Allanson JE, Gorlin's Syndromes of the Head and Neck. Fifth Edition, Oxford University Press, New York, USA, 2010.

Jeong J, Mao J, Tenzen T, Kottmann AH, McMahon AP. 2004. Hedgehog signaling in the neural crest cells regulates the patterning and growth of facial primordia. Genes Dev. 18(8):937-951.

Kawasaki M1, Porntaveetus T, Kawasaki K, Oommen S, Otsuka-Tanaka Y, Hishinuma M, Nomoto T, Maeda T, Takubo K, Suda T, Sharpe PT, Ohazama A. 2014. R-spondins/Lgrs expression in tooth development. Dev Dyn. 243(6):844-51.

Kim, J., Kato, M., Beachy, P.A., 2009. Gli2 trafficking links Hedgehog-dependent activation of Smoothened in the primary cilium to transcriptional activation in the nucleus. Proc. Natl. Acad. Sci. USA 106, 21666–21671.

Komatsu Y1, Yu PB, Kamiya N, Pan H, Fukuda T, Scott GJ, Ray MK, Yamamura K, Mishina Y.

2013. Augmentation of Smad-dependent BMP signaling in neural crest cells causes craniosynostosis in mice. J Bone Miner Res. 28(6):1422-33.

Liu B, Rooker SM, Helms JA. 2010. Molecular control of facial morphology. Semin Cell Dev Biol. 21(3):309-13.

Macca M, Franco B. 2009. The molecular basis of oral-facial-digital syndrome, type 1. Am J Med Genet C Semin Med Genet. 151C(4):318-25.

MacDonald ME, Hall BK. 2001. Altered timing of the extracellular-matrix-mediated epithelial-mesenchymal interaction that initiates mandibular skeletogenesis in three inbred strains of mice: development, heterochrony, and evolutionary change in morphology. J Exp Zool. 291(3):258-73.

Meikle MC. 1973. In vivo transplantation of the mandibular joint of the rat: an autoradiographic investigation into cellular changes at the condyle. Arch Oral Biol 18(8):1011–20.

Millington G, Elliott KH, Chang YT, Chang CF, Dlugosz A, Brugmann SA. 2017. Cilia-dependent GLI processing in neural crest cells is required for tongue development. Dev Biol. 424(2):124-137.

Mina M, Havens B, Velonis DA. 2007. FGF signaling in mandibular skeletogenesis. Orthod Craniofac Res. 10(2):59-66.

Murcia NS, Richards WG, Yoder BK, Mucenski ML, Dunlap JR, woychik RP. 2000. The Oak Ridge Polycystic Kidney (orpk) disease gene is required for leftright axis determination. Development 127(11): 2347–2355.

Ohazama A, Johnson EB, Ota MS, Choi HY, Porntaveetus T, Oommen S, Itoh N, Eto K, Gritli-Linde A, Herz J, Sharpe PT. 2008. Lrp4 modulates extracellular integration of cell signaling pathways in development. PLoS One. 3(12): e4092.

Oka K, Oka S, Sasaki T, Ito Y, Bringas P Jr, Nonaka K, Chai Y. 2007. The role of TGF-beta signaling in regulating chondrogenesis and osteogenesis during mandibular development. Dev Biol. 303(1):391-404.

Oka K, Oka S, Hosokawa R, Bringas P Jr, Brockhoff HC 2nd, Nonaka K, Chai Y. 2008. TGF-beta mediated Dlx5 signaling plays a crucial role in osteo-chondroprogenitor cell lineage determination during mandible development. Dev Biol. 5;321(2):303-9.

Paiva KB, Silva-Valenzuela Md, Massironi SM, Ko GM, Siqueira FM, Nunes FD. 2010. Differential Shh, Bmp and Wnt gene expressions during craniofacial development in mice. Acta Histochem. 112(5):508-17.

Pan J, Wang Q, Snell WJ. 2005. Cilium-generated signaling and cilia-related disorders. Lab Invest. 85(4):452-463.

Parada C, Chai Y. 2015. Mandible and Tongue Development. Curr Top Dev Biol. 115:31-58.

Rosenbaum JL, Witman GB. 2002. Intraflagellar transport. Nat Rev Mol Cell Biol. 3(Pt5):813-825,

Park HL, Bai C, Platt KA, Matise MP, Beeghly A, Hui CC, Nakashima M, Joyner AL. 2000. Mouse Gli1 mutants are viable but have defects in SHH signaling in combination with a Gli2 mutation. Development. 127(8):1593-605.

Sasai, N., Briscoe, J., 2012. Primary cilia and graded Sonic Hedgehog signaling. WIRES Dev. Biol., 753–772.

Shibata S, Sato R, Murakami G, Fukuoka H, Rodríguez-Vázquez JF. 2013. Origin of mandibular condylar cartilage in mice, rats, and humans: Periosteum or separate blastema? J Oral Biosci, 55: 208-216.

Shibata S, Suzuki S, Tengan T, Ishii M, Kuroda T. 1996. A histological study of the developing condylar cartilage of the fetal mouse mandible by using coronal sections. Arch Oral Biol 41(1):47–54.

Shibata S, Fukada K, Suzuki S, Yamashita Y. 1997. Immunohistochemistry of collagen types II and X, and enzyme-histochemistry of alkaline phosphatase in the developing condylar cartilage of the fetal mouse mandible. J Anat 191(Pt4): 561–70.

Singla V1, Romaguera-Ros M, Garcia-Verdugo JM, Reiter JF. 2010. Ofd1, a human disease gene, regulates the length and distal structure of centrioles. Dev Cell. 16;18(3):410-24

Symons NBB. 1952. The development of the human mandibular joints. J Anat 86:236–334.

Takahashi M, Tamura K, Buscher D, et al. The role of Alx-4 in the establishment of anteroposterior polarity during vertebrate limb development. Development. 1998;125:4417–4425.

Terao F, Takahashi I, Mitani H, Haruyama N, Sasano Y, Suzuki O, Takano-Yamamoto T. 2011. Fibroblast growth factor 10 regulates Meckel's cartilage formation during early mandibular morphogenesis in rats. Dev Biol. 15;350(2):337-47.

Thompson H, Ohazama A, Sharpe PT, Tucker AS. 2012. The origin of the stapes and relationship to the otic capsule and oval window. Dev Dyn. 241(9):1396-404.

Thompson H, Tucker AS. 2013. Dual origin of the epithelium of the mammalian middle ear. Science. 22;339(6126):1453-6.

Vendrell V1, Summerhurst K, Sharpe J, Davidson D, Murphy P. 2009. Gene expression

analysis of canonical Wnt pathway transcriptional regulators during early morphogenesis of the facial region in the mouse embryo. Gene Expr Patterns. 9(5):296-305.

Wang Y, Zheng Y, Chen D, Chen Y. 2013. Enhanced BMP signaling prevents degeneration and leads to endochondral ossification of Meckel's cartilage in mice. Dev Biol. 15;381(2):301-11.

Wang Y1, Liu C, Rohr J, Liu H, He F, Yu J, Sun C, Li L, Gu S, Chen Y. 2011. Tissue interaction is required for glenoid fossa development during temporomandibular joint formation. Dev Dyn. 240(11):2466-73.

Yi R, O'Carroll D, Pasolli HA, Zhang Z, Dietrich FS, Tarakhovsky A, Fuchs E. 2006. Morphogenesis in skin is governed by discrete sets of differentially expressed microRNAs. Nat Genet. 38(3):356-362.

Yuan X, Yang S. 2016. Primary Cilia and Intraflagellar Transport Proteins in Bone and Cartilage. J Dent Res. 95(12):1341-1349.

Zaghloul NA, Brugmann SA. 2011. The emerging face of primary cilia. Genesis. 49(4):231-246.

Zhang Z, Wlodarczyk BJ, Niederreither K, Venugopalan S, Florez S, Finnell RH, Amendt BA. 2011. Fuz regulates craniofacial development through tissue specific responses to signaling factors. PLoS One. 6(9):e24608.

Figure Legends

Figure 1. Mandibular bone phenotypes in *Ift88$^{fl/fl}$;Wnt1Cre* and *Ofd1^{fl};Wnt1Cre* mice

(A-C, G-I) Frontal sections showing the developing mandibular bone in wild-type (A, G), *Ofd1^{fl};Wnt1Cre* (B, H) and *Ift88$^{fl/fl}$;Wnt1Cre* (C, I) at E18.5 (A-C) and E13.5 (G-I). Blue arrow and arrowheads indicating wild-type endogenous lingual mandibular bone and mutant excess lingual mandibular bone, respectively (A-C). Arrowheads indicating ectopic condensed mesenchyme (H, I). (D-F) Caudal view of skeletal preparation of wild-type (D), *Ofd1^{fl};Wnt1Cre* (E) and *Ift88$^{fl/fl}$;Wnt1Cre* (F) at E18.5. Arrows indicating excess lingual mandibular bone. Yellow dotted lines indicating Meckel's cartilage. b: buccal side, l: lingual side. (J-L) Frontal sections showing *in situ* hybridization of *Runx2* in wild-type (J), *Ofd1^{fl};Wnt1Cre* (K) and *Ift88$^{fl/fl}$;Wnt1Cre* (L) at E13.5. Meckel's cartilage and tooth buds were outlined by red and yellow dots, respectively. Arrows indicating region corresponding ectopic bone. (M-O) Frontal sections showing BrdU positive cells in wild-type (M), *Ofd1^{fl};Wnt1Cre* (N) and *Ift88$^{fl/fl}$;Wnt1Cre* (O) at E12.5. Arrowheads indicating region corresponding ectopic bone. Meckel's cartilage was outlined by blue dots.

Figure 2. Shh signaling in mandibular bone development

Frontal sections showing *in situ* hybridization of *Ptch1* (A-C), *Sox9* (D), *Gli1* (F-H) and *Gli3* (L-N) and immunohistochemistry of Gli2 in wild-type (A, D, F, I, L), *Ofd1^{fl};Wnt1Cre* (B, G, , J, M) and *Ift88$^{fl/fl}$;Wnt1Cre* (C, H, K, N) at E12.5. Presumptive Meckel's cartilage region recognized by the presence of condensed mesenchymal cells was outlined by red dots. Yellow arrowheads indicating region corresponding ectopic bone. Red arrowheads indicating *Ptch1* and *Sox9* expression domain. (E, O, P) Frontal sections showing the developing mandibular bone in *Ofd1^{fl};Sox9Cre* (E), wild-type (O) and *Smo$^{fl/fl}$;Wnt1Cre* (P) at E18.5. Blue arrow and arrowheads indicating wild-type endogenous mandibular bone and mutant excess lingual mandibular bone, respectively. (Q, R) Caudal view of skeletal preparation of wild-type (Q) and *Smo$^{fl/fl}$;Wnt1Cre* (R) at E18.5. Yellow arrows indicating lingual region of mandibular bone. Yellow dotted lines indicating Meckel's cartilage. b: buccal side, l: lingual side. (S, T) Frontal sections showing *in situ* hybridization of *Runx2* in wild-type (S) and *Smo$^{fl/fl}$;Wnt1Cre* (T) at E13.5. Meckel's cartilage was outlined by red dots. Arrows indicating region corresponding ectopic bone.

Figure 3. *Gli3* in mandibular bone development

Frontal sections showing the developing mandibular bone in wild-type (A) and *Gli3* mutant mice (B) at E18.5. Arrows indicating lingual region of mandibular bone.

Figure 4. Meckel's cartilage phenotypes in *Ift88$^{fl/fl}$;Wnt1Cre* and *Ofd1^{fl};Wnt1Cre* mice

(A-C, G-I) Frontal sections showing the developing posterior Meckel's cartilage in wild-type (A, G), *Ofd1^{fl};Wnt1Cre* (B, H) and *Ift88$^{fl/fl}$;Wnt1Cre* (C, I) at E18.5 (A-C) and E14.5 (G-I). Meckel's cartilage was outlined by blue dots. Arrowheads indicating thickened pericondrium. (D-F) 3D reconstruction of Meckel's cartilage of wild-type (D), *Ofd1^{fl};Wnt1Cre* (E) and *Ift88$^{fl/fl}$;Wnt1Cre* (F) at E14.5. Arrows indicating molar region.

Figure 5. Shh signaling in Meckel's cartilage formation

(A-I) Frontal sections showing *in situ* hybridization of *Gli1* (A-C) and *Gli3* (G-I), and immunohistochemistry of Gli2 (D-F) in wild-type (A, D, G), *Ofd1^{fl};Wnt1Cre* (B, E, H) and *Ift88$^{fl/fl}$;Wnt1Cre* (C, F, I) at E13.5. Meckel's cartilage was outlined by red dots. (J, K, N, O) Frontal sections showing the developing Meckel's cartilage in wild-type (J, N), *Smo$^{fl/fl}$;Wnt1Cre* (K) and *Ofd1^{fl};Sox9Cre* (O) at E18.5. Meckel's cartilage was outlined by blue dots. (L, M) 3D reconstruction of Meckel's cartilage of wild-type (L) and *Smo$^{fl/fl}$;Wnt1Cre* (M) at E14.5.

Figure 6. Proximal end of mandibles and ossicles in *Ift88$^{fl/fl}$;Wnt1Cre*, *Ofd1^{fl};Wnt1Cre* and *Smo$^{fl/fl}$;Wnt1Cre* mice

(A-D) Proximal end of skeletal preparation of wild-type (A), *Ofd1$^{fl/Y}$;Wnt1Cre* (B), *Ift88$^{fl/fl}$;Wnt1Cre* (C) and *Smo$^{fl/fl}$;Wnt1Cre* (D) at E18.5. Arrows indicating extra cartilage formation. (E-H) Frontal sections showing the developing condylar and glenoid fossa region in wild-type (E), *Ofd1^{fl};Wnt1Cre* (F), *Ift88$^{fl/fl}$;Wnt1Cre* (G) and *Smo$^{fl/fl}$;Wnt1Cre* (H) at E18.5. Arrows indicating glenoid fossa region. (I-L) Lateral view of Alcial blue stained ossicles of wild-type (I), *Ofd1^{fl};Wnt1Cre* (J), *Ift88$^{fl/fl}$;Wnt1Cre* (K) and *Smo$^{fl/fl}$;Wnt1Cre* (L) at E18.5.

Figure 7. Mandiblular bone and Meckel's cartilage in *Ofd1^{fl};Ift88$^{fl/fl}$;Wnt1Cre* mice

Frontal sections showing the developing mandibular bone and Meckel's cartilage in wild-type (A, C) and *Ofd1^{fl};Ift88$^{fl/fl}$;Wnt1Cre* (B, D) at E18.5. Arrow and arrowheads indicating wild-type endogenous mandibular bone and excess lingual mandibular bone, respectively. Meckel's cartilage was outlined by blue dots.

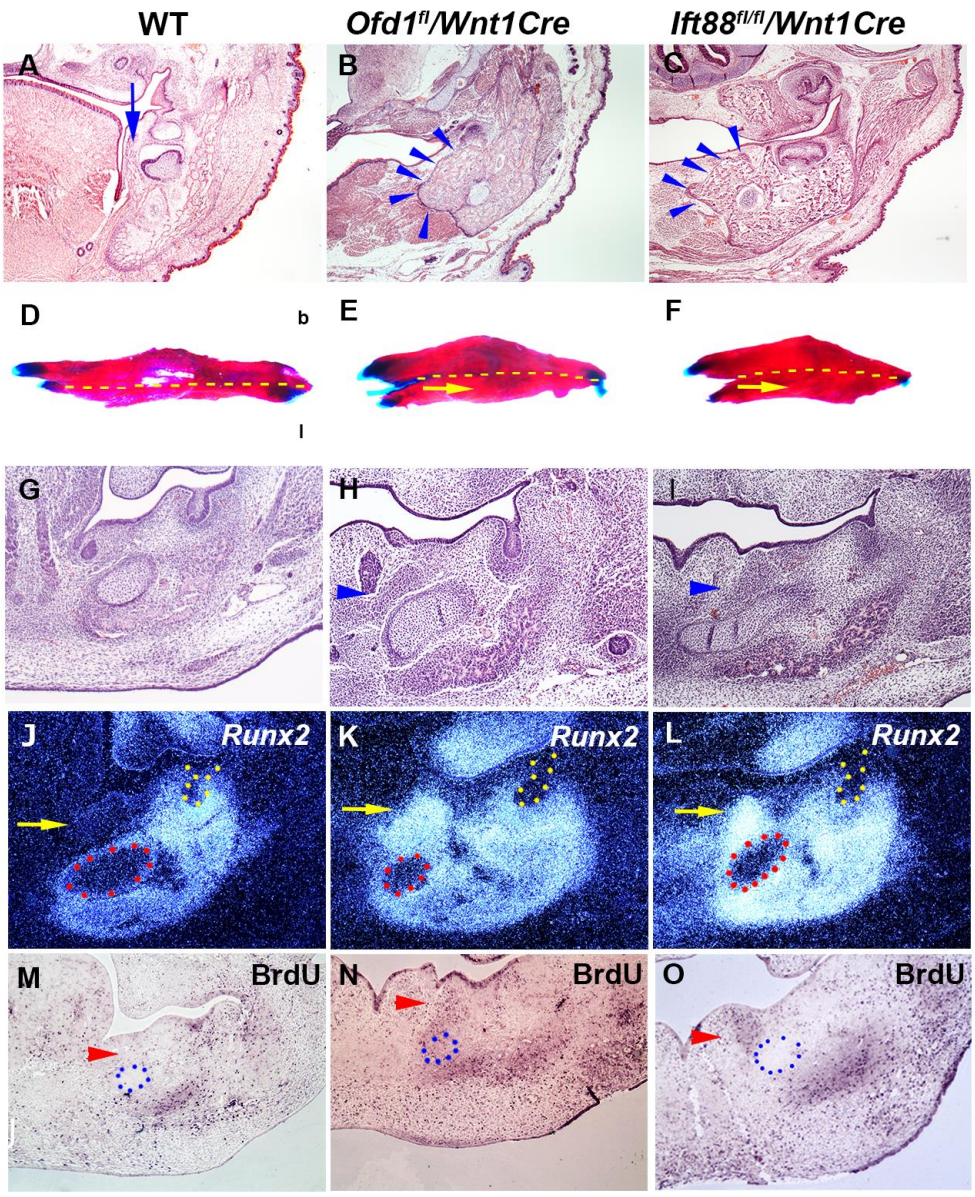
WT
Ofd1fl/Wnt1Cre
Ift88fl/fl/Wnt1Cre
A
B
C
D
b
l
E
F
G
H
I
J
Runx2
K
Runx2
L
Runx2
M
BrdU
N
BrdU
O
BrdU

Figure 1

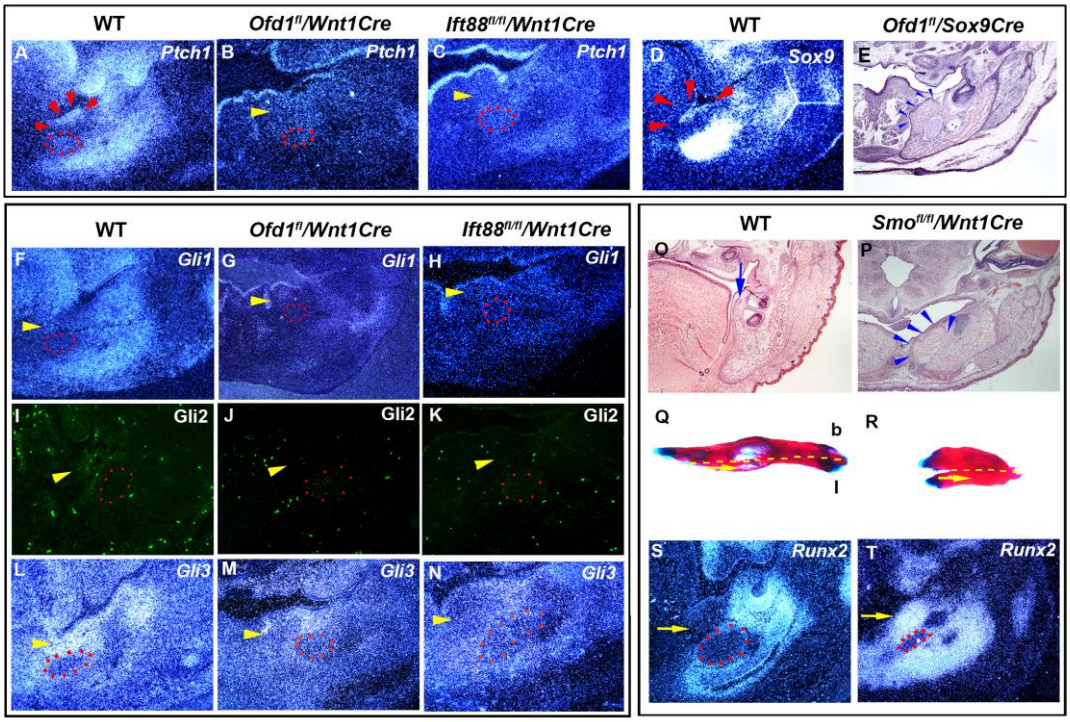
WT
Ofd1fl/Wnt1Cre
Ift88fl/fl/Wnt1Cre
WT
Ofd1fl/Sox9Cre
A Ptch1
B Ptch1
C Ptch1
D Sox9
E
WT
Ofd1fl/Wnt1Cre
Ift88fl/fl/Wnt1Cre
F Gli1
G Gli1
H Gli1
I Gli2
J Gli2
K Gli2
L Gli3
M Gli3
N Gli3
WT
Smofl/fl/Wnt1Cre
O
P
Q
b
l
R
S Runx2
T Runx2

Figure 2

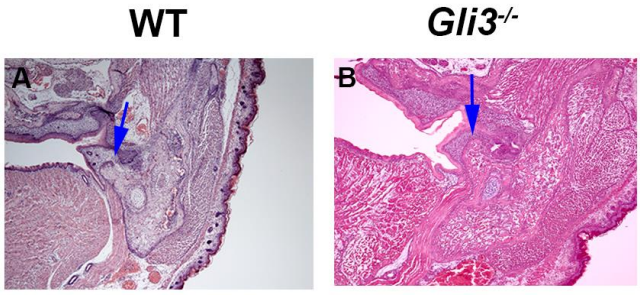

Figure 3

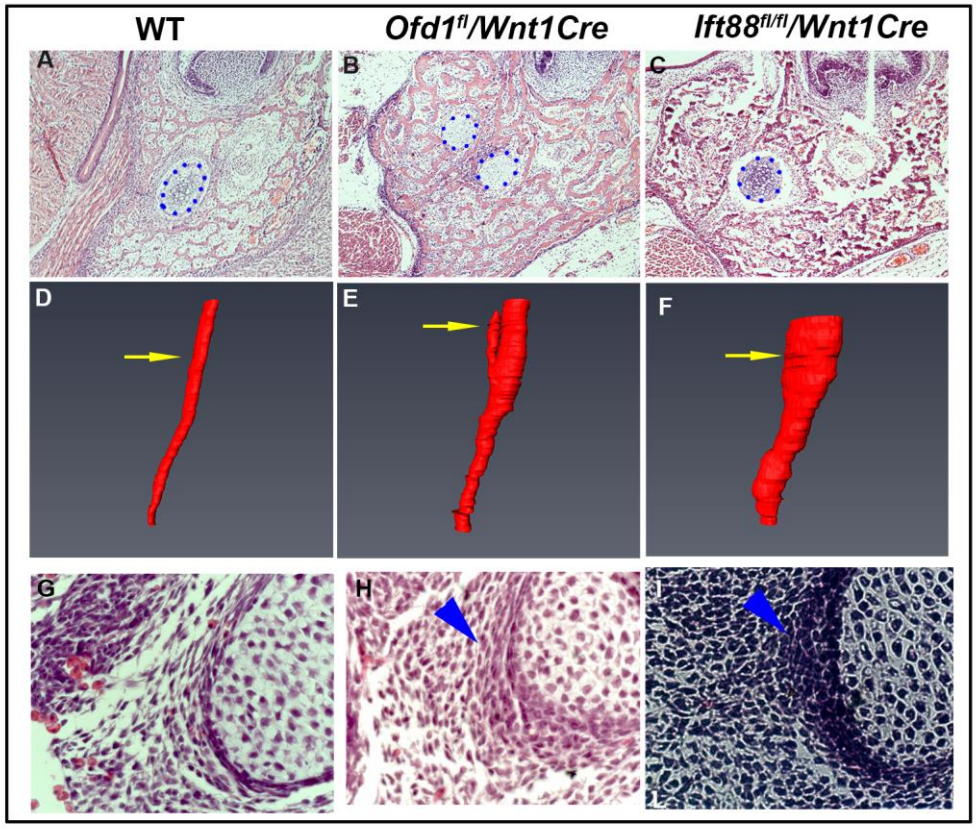

Figure 4

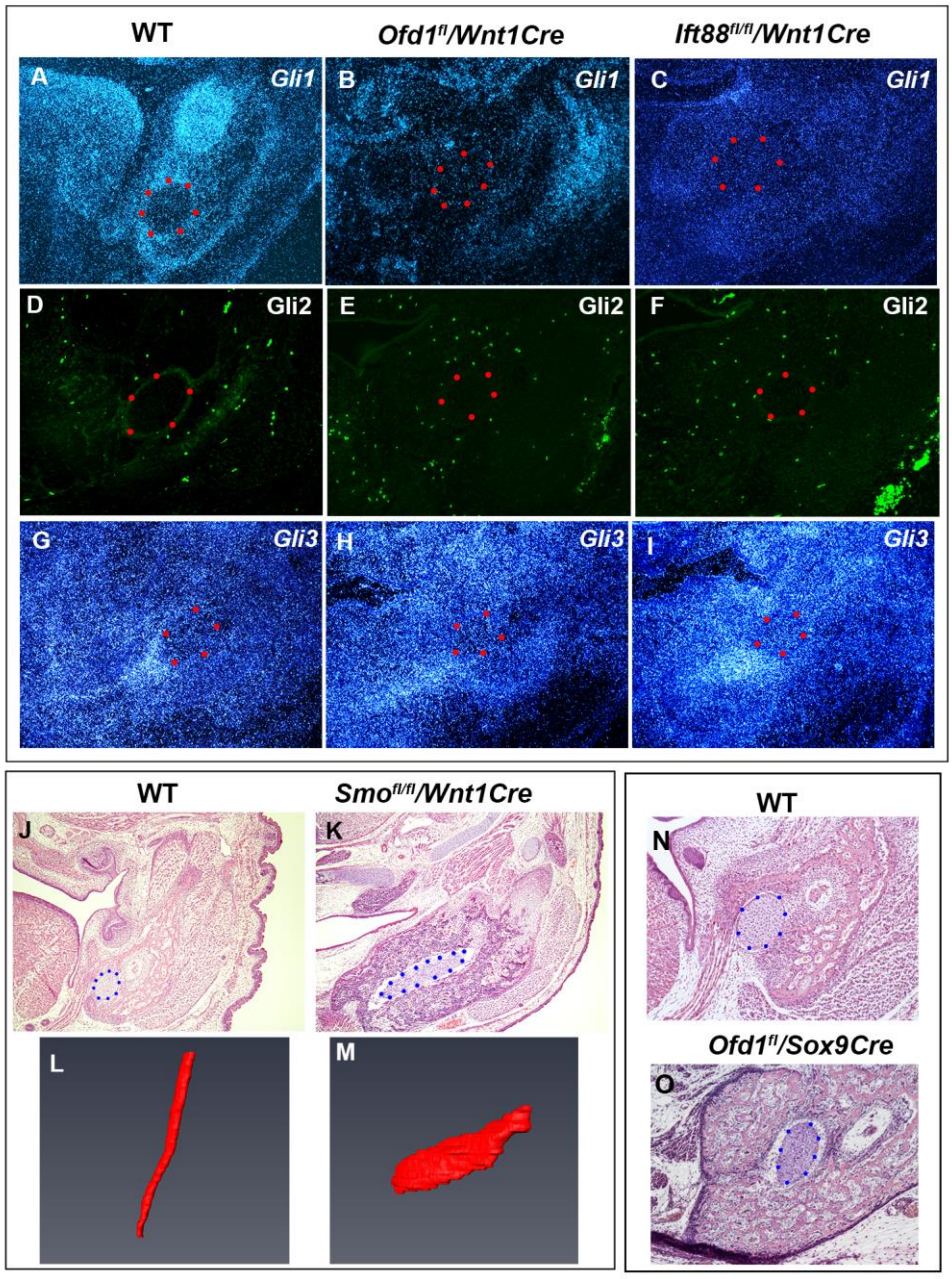
WT
Ofd1fl/Wnt1Cre
Ift88fl/fl/Wnt1Cre
A
Gli1
B
Gli1
C
Gli1
D
Gli2
E
Gli2
F
Gli2
G
Gli3
H
Gli3
I
Gli3
WT
Smofl/fl/Wnt1Cre
J
K
L
M
WT
N
Ofd1fl/Sox9Cre
O

Figure 5

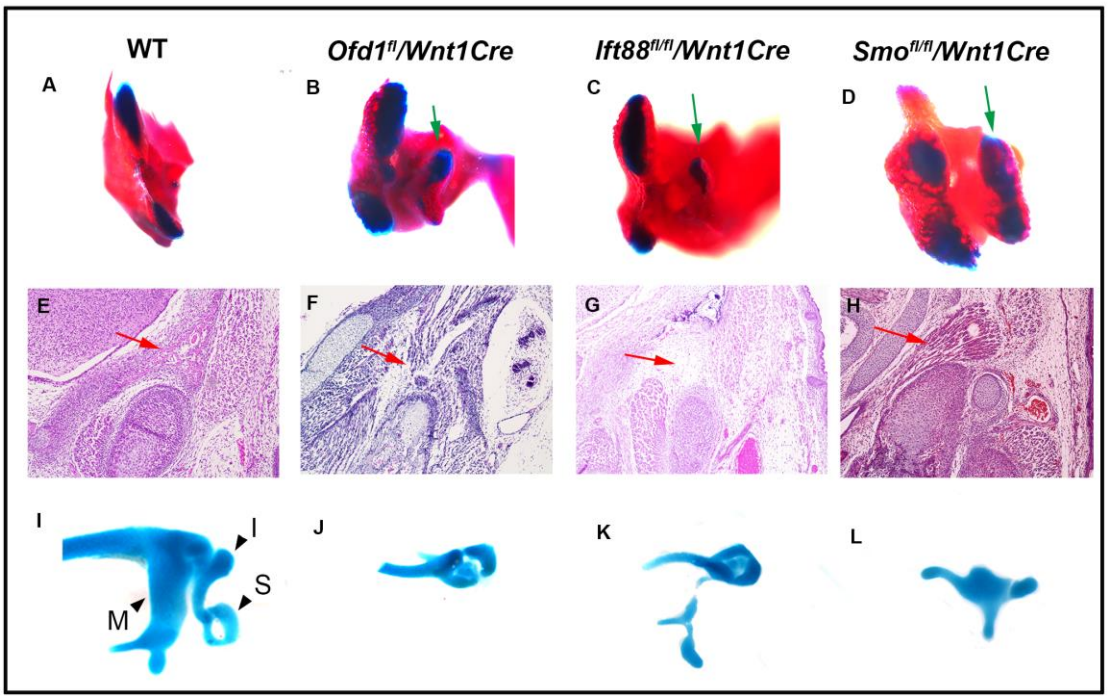
WT
Ofd1fl/Wnt1Cre
Ift88fl/fl/Wnt1Cre
Smofl/fl/Wnt1Cre
A
B
C
D
E
F
G
H
I
J
K
L
I
S
M

Figure 6

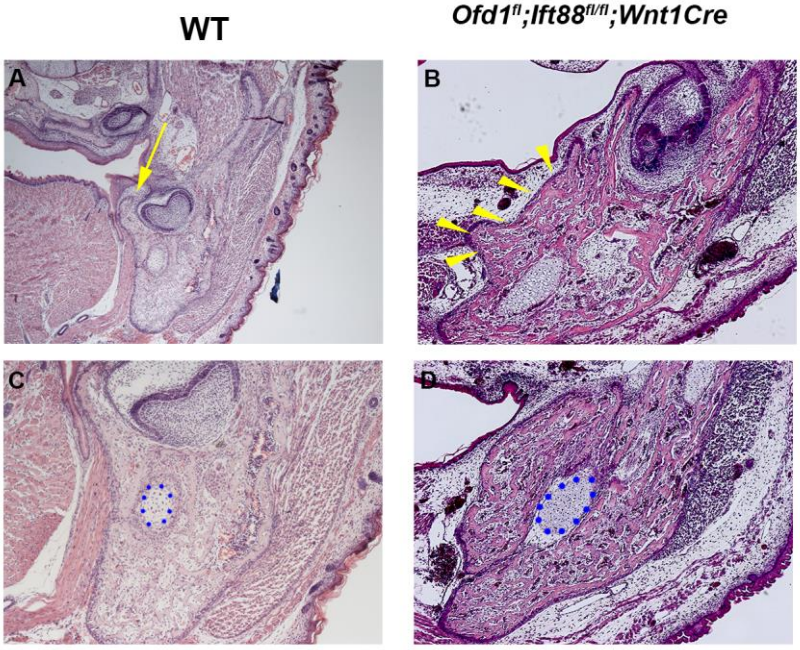

Figure 7